9th AIAA Aviation Technology, Integration, and Operations Conference (ATIO)
and
Air
21 - 23 September 2009, Hilton Head, South Carolina

AIAA 2009-6951

Exploiting Patterns in the Kulfan Transformations of Supercritical Airfoils

András Sóbester*
University of Southampton, Southampton, Hampshire, SO17 1BJ, UK

For a parametric airfoil to be genuinely useful in preliminary design optimization it has to satisfy a number of requirements. Perhaps most importantly the number of design variables has to be small and the design space defined by them has to exclude geometrically unrealistic shapes. Ideally, the design variables should also have intuitive significance, that is, they should be directly linked to geometrical or aerodynamic features. Furthermore, it is advantageous to have a multi-level parameterisation built into the same mathematical form, to allow design searches with increasing level of detail. Here we propose two general methods for generating airfoils that satisfy these criteria by exploiting certain patterns in the Kulfan (or class-shape function) transformations of families of existing airfoils. We illustrate the two methods by constructing concise parametric airfoils based on the NASA SC(2) family of supercritical sections.

I. Parametric Airfoils in Preliminary Design

THE cost of exploring a design space increases exponentially with the number of design variables. This *curse of dimensionality* is particularly pressing in the context of preliminary design, where the desire to explore a wide range of configurations may tempt the engineer into equipping the parametric airframe geometry with numerous degrees of freedom. These, through their often counter-intuitively drastic effect on the complexity of the design problem, then risk bringing about the peril of restricting any reasonable MDO (Multidisciplinary Design Optimization) process to merely scratching the surface of the (unnecessarily inflated) design space. The desire for new design variables driven by the need for flexibility must therefore be tempered by an understanding of *necessary* flexibility. The specific problem we tackle here is that of airfoil design, so let us consider an example from this fundamental problem class.

Few would dispute that if the design brief calls for a long range airliner with a cruise Mach number of 0.8, there is little point in equipping the parametric airfoil with degrees of freedom that will enable it to reproduce highly cambered sections. There is, however, a school of thought according to which it is worth adding more flexibility to a scheme that can produce suitable (in this example, supercritical) shapes (say, by inserting additional control points into a NURBS airfoil), because the new scheme will no doubt be capable of producing *additional* suitable shapes, as well as clearly inappropriate ones, which are merely seen as a byproduct of the process. Our thesis here is two-fold. On the one

*Lecturer, Computational Engineering and Design Group, AIAA member.

hand this is a very expensive byproduct: an automated optimization process will not 'know' that there is no point in running the expensive numerical multidisciplinary analysis over something that an aerodynamicist would recognize as a low Reynolds/Mach number section (or worse still, a completely nonsensical one) when looking for a Mach 0.8 design – therefore many evaluations may get wasted. On the other hand, once the global search is complete (on the more restricted, but very concise foil), there is still scope for a *local* search in the vicinity of the optimum, over a re-parameterised airfoil. We reviewed some possible schemes for such a local re-parameterisation in Ref. 1 – one example is the mesh-based formulation of Jameson,[2] designed specifically for local optimization guided by adjoint flow solutions.

Of course, the initial, parsimonious parameterization has to be flexible enough to enable a meaningful global search in the context of the problem at hand. Here we argue that one way of achieving this, while limiting the design space to a problem-specific 'sensible' region, is to approximate a diverse set of existing, suitable 'training' geometries through some highly generic model and then build the problem-specific model based on patterns detected in the parameters of the generic descriptor.

The idea of exploiting the features of a tried and tested family of airfoils by blending them into a parametric representation is not without precedent. In fact, the orthogonal basis functions introduced by Robinson and Keane[3] are based on the very same class of shapes we are using here: SC(2), the second generation of NASA supercritical airfoils (much more on which later). Supercritical airfoils of various classes were used as bases in Ref. 1, where very concisely parameterized NURBS (Non-Uniform Rational B-Spline) representations were defined in the reduced order space of the bases*.

Here we describe a recipe for building a very concise model by capturing the shapes of the members of a family through a highly flexible approximation model (Kulfan's Class-Shape Function transformation – described in the next Section) and, by exploiting family-specific patterns in the variables of these approximations (Sections IV and V), establishing a mapping between these and a those of a much more concise parametric shape. We show through an example [that of the already mentioned CS(2) family, described in detail in Section III] how, beyond the dimensionality reduction, as an added bonus, the parameters of the concise airfoil can be chosen such that they are linked to the known physical properties of the members of the family. We conclude this study by reflecting on the place of these findings in the context of the overall aerodynamic design process (Section VI) and on possible future developments (Section VII).

II. Airfoil Shape Approximation via Kulfan (Class-Shape Function) Transformation

In what follows we shall use a coordinate system whose x axis is aligned with the chord, with the leading edge point in the origin and the trailing edge point(s) at $x = 1$. We define a universal approximation to any airfoil in the xOz plane as a pair of explicit curves $\mathcal{A} = [z^{\mathrm{u}}(x, \ldots), z^{\mathrm{l}}(x, \ldots)]$, where $x \in [0, 1]$ and the superscripts u and l distinguish between the upper and the lower surface (here and on all the symbols in the following discussion) and the dots indicate that the shape of the two curves depends on a number of parameters. $\mathcal{A}$ becomes the approximation to a target airfoil if

*See Refs. 4, 5 for further instances of parameterisation using basis airfoils.

we determine these parameters such that they minimize some metric of difference (say, mean squared error) between $\mathcal{A}$ and the target.

As indicated in the introduction, numerous such generic airfoil description templates exist – here we adopt the class-shape transformation of Kulfan.[6] The main traits that make this scheme attractive for our purposes are its ability a) to approximate practically any airfoil (flexibility) and b) to require a relatively small number of design variables do so with high accuracy (conciseness) – see Ref. 7 for the empirical and analytical underpinning of this.

Let the generic airfoil be defined as

$$\begin{aligned}\mathcal{A}(\mathbf{V}) &= \mathcal{A}[x,\ v_0^{\mathrm{u}}, v_1^{\mathrm{u}}, \dots v_{n_{\mathrm{BP}}^{\mathrm{u}}}^{\mathrm{u}}, z_{\mathrm{TE}}^{\mathrm{u}}, v_{\mathrm{LE}}^{\mathrm{u}},\ v_0^{\mathrm{l}}, v_1^{\mathrm{l}}, \dots v_{n_{\mathrm{BP}}^{l}}^{\mathrm{l}}, z_{\mathrm{TE}}^{\mathrm{l}}, v_{\mathrm{LE}}^{\mathrm{l}}] = \\ &= [z^{\mathrm{u}}(x, v_0^{\mathrm{u}}, v_1^{\mathrm{u}}, \dots v_{n_{\mathrm{BP}}^{\mathrm{u}}}^{u}, z_{\mathrm{TE}}^{\mathrm{u}}, v_{\mathrm{LE}}^{\mathrm{u}}),\ z^{\mathrm{l}}(x, v_0^{\mathrm{l}}, v_1^{\mathrm{l}}, \dots v_{n_{\mathrm{BP}}^{\mathrm{l}}}^{\mathrm{l}}, z_{\mathrm{TE}}^{\mathrm{l}}, v_{\mathrm{LE}}^{\mathrm{l}})],\end{aligned} \tag{1}$$

where n_{BP}^{u} and n_{BP}^{l} denote the orders of sets of Bernstein polynomials that control the shape of the two curves that make up the airfoil. The upper surface of the airfoil is defined as:

$$\begin{aligned}z^{\mathrm{u}}(x,\ v_0^{\mathrm{u}}, v_1^{\mathrm{u}}, \dots v_{n_{\mathrm{BP}}^{\mathrm{u}}}^{\mathrm{u}}, z_{\mathrm{TE}}^{\mathrm{u}}, v_{\mathrm{LE}}^{\mathrm{u}}) = \underbrace{\sqrt{x}(1-x)}_{\text{class function}} \underbrace{\sum_{r=0}^{n_{\mathrm{BP}}^{\mathrm{u}}} v_r^{\mathrm{u}}\ C_{n_{\mathrm{BP}}^{\mathrm{u}}}^{\ r} x^r (1-x)^{n_{\mathrm{BP}}^{\mathrm{u}}-r}}_{\text{scaled Bernstein partition of unity}} + \\ + \underbrace{z_{\mathrm{TE}}^{u} x}_{\text{trailing edge thickness term}} + \\ + \underbrace{x\sqrt{1-x}\ v_{\mathrm{LE}}^{\mathrm{u}}(1-x)^{n_{\mathrm{BP}}^{\mathrm{u}}}}_{\text{supplementary leading edge shaping term}},\end{aligned} \tag{2}$$

where $C_{n_{\mathrm{BP}}^{\mathrm{u}}}^{\ r} = \frac{n_{\mathrm{BP}}^{\mathrm{u}}!}{r!(n_{\mathrm{BP}}^{\mathrm{u}}-r)!}$. A curve built upon the same template defines the lower surface:

$$\begin{aligned}z^{\mathrm{l}}(x,\ v_0^{\mathrm{l}}, v_1^{\mathrm{l}}, \dots v_{n_{\mathrm{BP}}^{\mathrm{l}}}^{\mathrm{l}}, z_{\mathrm{TE}}^{\mathrm{l}}, v_{\mathrm{TE}}^{\mathrm{l}}) = \underbrace{\sqrt{x}(1-x)}_{\text{class function}} \underbrace{\sum_{r=0}^{n_{\mathrm{BP}}^{\mathrm{l}}} v_r^{\mathrm{l}}\ C_{n_{\mathrm{BP}}^{\mathrm{l}}}^{\ r} x^r (1-x)^{n_{\mathrm{BP}}^{\mathrm{l}}-r}}_{\text{scaled Bernstein partition of unity}} + \\ + \underbrace{z_{\mathrm{TE}}^{\mathrm{l}} x}_{\text{trailing edge thickness term}} + \\ + \underbrace{x\sqrt{1-x}\ v_{\mathrm{LE}}^{\mathrm{l}}(1-x)^{n_{\mathrm{BP}}^{\mathrm{l}}}}_{\text{supplementary leading edge shaping term}}.\end{aligned} \tag{3}$$

Approximating an arbitrary smooth airfoil with these expressions amounts to finding the vectors

$$\mathbf{v}^{\mathrm{u}} = \{ \overbrace{v_0^{\mathrm{u}}, v_1^{\mathrm{u}}, \dots v_{n_{\mathrm{BP}}^{\mathrm{u}}}^{\mathrm{u}}, v_{\mathrm{LE}}^{\mathrm{u}}}^{n_{\mathrm{BP}}^{\mathrm{u}}+2 \text{ design variables to define upper surface}} \}^{\mathrm{T}} \tag{4}$$

and

$$\mathbf{v}^{\mathrm{l}} = \{ \overbrace{v_0^{\mathrm{l}}, v_1^{\mathrm{l}}, \dots v_{n_{\mathrm{BP}}^{\mathrm{l}}}^{\mathrm{l}}, v_{\mathrm{LE}}^{\mathrm{l}}}^{n_{\mathrm{BP}}^{\mathrm{l}}+2 \text{ design variables to define lower surface}} \}^{\mathrm{T}} \tag{5}$$

(note that z^u_{TE} and z^l_{TE} are simply the trailing edge ordinates of the target airfoil so they are known) which, as indicated earlier, minimize some metric of the difference between $\mathcal{A}(\mathbf{V})$ and the target airfoil.

Let us consider, say, the upper surface of a target airfoil, given as a list of $n^{\mathrm{u}}_{\mathrm{T}}$ coordinate pairs $\left\{(x^{\mathrm{u}}_{\mathrm{T}i}, z^{\mathrm{u}}_{\mathrm{T}i})\,|i = \overline{1, n^{\mathrm{u}}_{\mathrm{T}}}\right\}$. We can exploit the linearity (in terms of the design variables) of the Kulfan approximation by re-arranging Equation (2) in matrix form, equating each of these target points with their approximations:

$$\mathbf{B}^{\mathrm{u}}.\mathbf{v}^{\mathrm{u}} = \mathbf{z}^{\mathrm{u}}, \tag{6}$$

where $\mathbf{z}^{\mathrm{u}} = \left\{z^{\mathrm{u}}_{\mathrm{T}1} - z^{\mathrm{u}}_{\mathrm{TE}}x^{\mathrm{u}}_{\mathrm{T}1},\ z^{\mathrm{u}}_{\mathrm{T}2} - z^{\mathrm{u}}_{\mathrm{TE}}x^{\mathrm{u}}_{\mathrm{T}2},\ \ldots\ z^{\mathrm{u}}_{\mathrm{T}n^{\mathrm{u}}_{\mathrm{T}}} - z^{\mathrm{u}}_{\mathrm{TE}}x^{\mathrm{u}}_{\mathrm{T}n^{\mathrm{u}}_{\mathrm{T}}}\right\}^{\mathrm{T}}$ and $\mathbf{B}^{\mathrm{u}}$ is an $n^{\mathrm{u}}_{\mathrm{T}} \times (n^u_{\mathrm{BP}} + 2)$ matrix of the class-shape function transformation terms, comprising the Bernstein polynomials

$$\mathbf{B}_{p,q} = \sqrt{x^{\mathrm{u}}_{\mathrm{Tp}}}(1 - x^{\mathrm{u}}_{\mathrm{Tp}})C^{q-1}_{n^u_{\mathrm{BP}}}{x^u_{\mathrm{Tp}}}^{q-1}(1 - x^{\mathrm{u}}_{\mathrm{Tp}})^{n^{\mathrm{u}}_{\mathrm{BP}}-q+1},\ p = \overline{1, n^{\mathrm{u}}_{\mathrm{T}}},\ q = \overline{1, n^{\mathrm{u}}_{\mathrm{BP}} + 1} \tag{7}$$

and the leading edge shaping terms

$$\mathbf{B}_{p,n_{\mathrm{BP}}+2} = x^{\mathrm{u}}_{\mathrm{Tp}}\sqrt{(1 - x^{\mathrm{u}}_{\mathrm{Tp}})}(1 - x^{\mathrm{u}}_{\mathrm{Tp}})^{n^u_{\mathrm{BP}}},\ p = \overline{1, n^{\mathrm{u}}_{\mathrm{T}}}. \tag{8}$$

Computing $\mathbf{v}^{\mathrm{u}} = \mathbf{B}^{\mathrm{u}+}\mathbf{z}^{\mathrm{u}}$ (where $\mathbf{B}^{\mathrm{u}+} = \left(\mathbf{B}^{\mathrm{u}\mathrm{T}}\mathbf{B}^{\mathrm{u}}\right)^{-1}\mathbf{B}^{\mathrm{u}\mathrm{T}}$ is the Moore-Pennrose pseudo-inverse of $\mathbf{B}^{\mathrm{u}}$) will now yield the set of coefficients that correspond to a least squares fit through the points of the target airfoil. Naturally, the same procedure can be repeated for the lower surface.

The accuracy of any such approximation can be improved by increasing the orders $n^{\mathrm{u}}_{\mathrm{BP}}$ and $n^{\mathrm{l}}_{\mathrm{BP}}$ of the Bernstein polynomials, thus adding more shaping terms (see Ref. 7 for experiments illustrating this on a range of airfoils). Generally, few applications require orders greater than about seven or eight and in many cases fewer terms are needed to approximate the upper surface of a cambered airfoil than the lower.

In what follows, when referring to the class-shape function approximation of an airfoil, we shall add the name of that airfoil to the previously introduced notation as a subscript, preceded by a '$\sim$' symbol to indicate the inexact nature of the approximation. Thus, for example, we shall refer to the the class-shape approximation of the supercritical airfoil SC(2)-0612 as

$$\mathcal{A}_{\sim\mathrm{SC}(2)-0612} = \mathcal{A}(\mathbf{V}_{\sim\mathrm{SC}(2)-0612}) = \mathcal{A}[v^{\mathrm{u}}_{0\sim\mathrm{SC}(2)-0612}, v^{\mathrm{u}}_{1\sim\mathrm{SC}(2)-0612}, \ldots v^{\mathrm{l}}_{\mathrm{LE}\sim\mathrm{SC}(2)-0612}]. \tag{9}$$

Figure 1 depicts the terms of this approximation for $n^u_{\mathrm{BP}} = 2$ and $n^l_{\mathrm{BP}} = 3$. As per equations (2) and (3), the total number of degrees of freedom (design variables) for this approximation is $n^u_{\mathrm{BP}} + 2 + n^l_{\mathrm{BP}} + 2 = 9$.

III. The SC(2) Family of Supercritical Airfoils – Origins and Analysis

The SC(2) Family of Supercritical Airfoils is the result of research conducted by NASA starting in the 1960s aimed at the development of "practical airfoils with two-dimensional transonic turbulent flow and improved drag divergence Mach numbers while retaining acceptable low-speed maximum lift and stall characteristics".[8] They trace their lineage back to the work of Whitcomb and Clark,[9] who

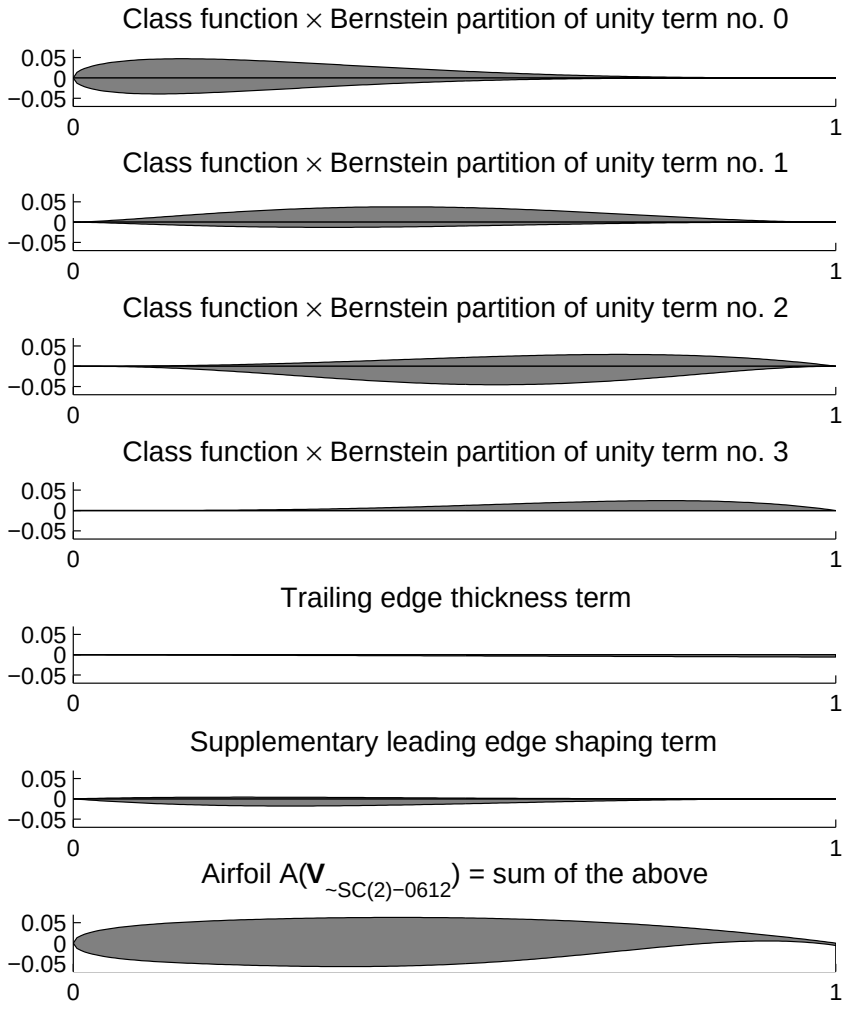

Fig. 1 The terms of equations (2) and (3) making up the class-shape approximation of the supercritical airfoil SC(2)-0612. Note that there is a single term no. 3, as we have used fewer polynomial terms to describe the upper surface and that, somewhat counter-intuitively, the sole term present there is, in fact, a positive one, though it participates in the approximation of the negative, lower surface.

noted that a three quarter chord slot between the upper an lower surfaces of a NACA 64A series airfoil gave it the ability to operate efficiently at Mach numbers greater than its original critical Mach number – hence the term 'supercritical', or 'SC' for short. The number in brackets following the 'SC' designation places each of these 'family-related' airfoils (to use Harris's term[8]) into one of three distinct phases of development through the 1970s and 1980s.

The fundamental design philosophy of the SC airfoils was to delay drag rise on the top surface through a reduction in curvature in the middle region, in order to reduce flow acceleration and thus reduce the local Mach number. This, in turn, reduces the severity of the adverse pressure gradient there and thus the associated shock is moved aft and is weakened. From a purely aerodynamic standpoint, the idea was to create a flat top pressure profile forward of the shock, obtained by balancing the expansion waves emanating from the leading edge, the compression waves resulting from their reflection off the sonic line (separating the subsonic and supersonic flow regions) back onto the surface and a second set of expansion waves associated with their reflection. Geometrically, this was achieved through a large leading edge radius (strong expansion waves) and a flat mid-chord region (reducing the accelerations that would have needed to be overcome by the reflected compression waves).[10] The well-known lower surface aft-end 'cusp' of the SC class of airfoils is a result of efforts to increase circulation, which led to a relatively aggressive aft-loading on the airfoil, as well as to the attainment of the design lift coefficients at low angles of attack.

Of all the NASA SC airfoils the SC(2) series has shown the greatest longevity and it forms the focus of the present study. It comprises 21 airfoils of different thickness to chord ratios and design lift coefficients. The first two digits of the encoding of each airfoil represent the design lift coefficient (multiplied by ten), while the third and the fourth digit represent the maximum thickness to chord ratio (as a percentage). Thus, for instance, SC(2)-0714 is the 14% thick second series supercritical airfoil designed for a lift coefficient of 0.7.

The design Reynolds numbers for airfoils with a thickness to chord ratio of 6% or greater were between 30×10^6 and 40×10^6, while the thinner airfoils were designed for $Re = 10 \times 10^6$. As a result of the geometrical features outlined above the design point angle of attack is expected to be close to zero at a speed in the region of the point where the the slope of the drag versus Mach number curve passes 0.1 (drag divergence).[8]

IV. Exploiting Shared Features

Let us consider six of the 21 members of the SC(2) family, all designed for transport aircraft: SC(2)-0410, SC(2)-0610, SC(2)-0710, SC(2)-0412, SC(2)-0612 and SC(2)-0712. Following the formulation described in Section II, we approximate these airfoils using the class-shape function transformation based on the Bernstein partitions of unity[†] of orders $n^{\mathrm{u}}_{\mathrm{BP}} = 5$ and $n^{\mathrm{l}}_{\mathrm{BP}} = 5$. This means that we have to find the 12 polynomial coefficients (6 for each surface) plus an additional leading edge shaping term for each surface, that minimizes the difference (mean squared error) between the approximation and the target. We take the trailing edge parameters $z^{\mathrm{u}}_{\mathrm{TE}}$ and $z^{\mathrm{l}}_{\mathrm{TE}}$ to be equal to the trailing edge thicknesses of the given target airfoil, so, of the total of 16 approximation parameters, we are left with

[†]So called because the terms of the series add up to one, regardless of the order.

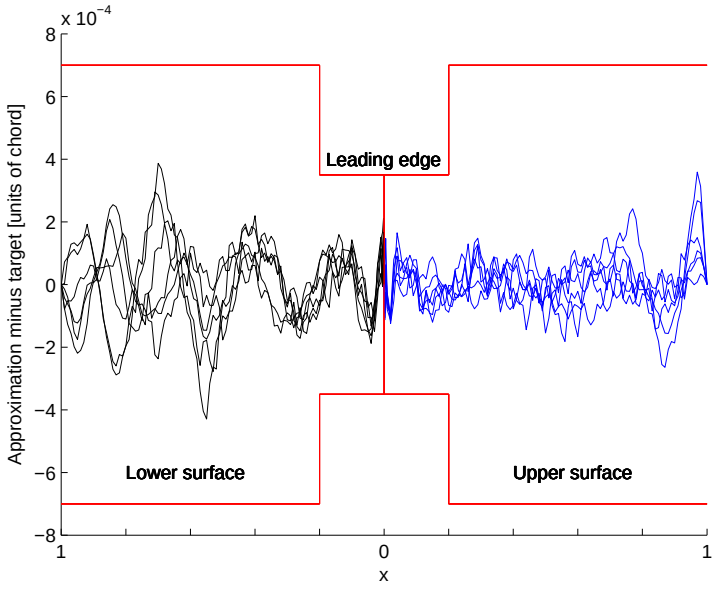

Fig. 2 Approximation errors: the differences between the six supercritical airfoils and their class-shape transformations. The horizontal lines indicate the typical tolerances of wind tunnel models (tighter within 20% chord of the leading edge).

14 to be determined.

Figure 2 illustrates the accuracy of the approximations we have found, indicating that the approximation errors are well within the typical tolerances of wind tunnel models ($\pm 3.5 \times 10^{-4}$ units of chord within 20% of the leading edge and $\pm 7 \times 10^{-4}$ elsewhere).

We thus have a 16 dimensional design space inhabited by six designs with, as yet, no obvious connection between them. For a parameterization that is more useful from a preliminary design perspective, we now seek to construct a reduced dimensionality space, which we can map back into this original domain, or, more accurately, into the sub-domain delimited by the six examples. One way of achieving this is to identify common features the members of this family of six sections share.

A. Divide and Conquer

Consider, the thickness distributions of our six chosen airfoils. As seen in Figure 3, the airfoils with the same maximum thickness to chord ratios share, in fact, their entire thickness distributions. Clearly, therefore, the different design lift coefficients are purely down to the different camber curve shapes (Figure 4) and this is good news from the perspective of mapping to a more concise description. We can apply the *divide and conquer* principle by separating, in terms of transformation coefficients, the effects of the two features that headline each of the SC(2) airfoils, design lift coefficient (clearly determined by the shape of the camber curve) and maximum thickness to chord ratio (determined by the thickness distribution). It also gives us a strong indication that, of all the possible variables we could use, it makes most sense to define the new, concise design space in terms of maximum thickness

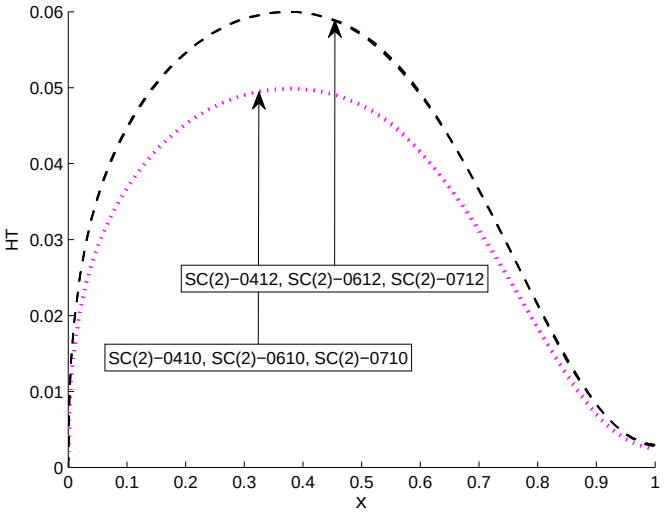

Fig. 3 The half-thickness distributions of the six SC(2) airfoils (axes to different scales).

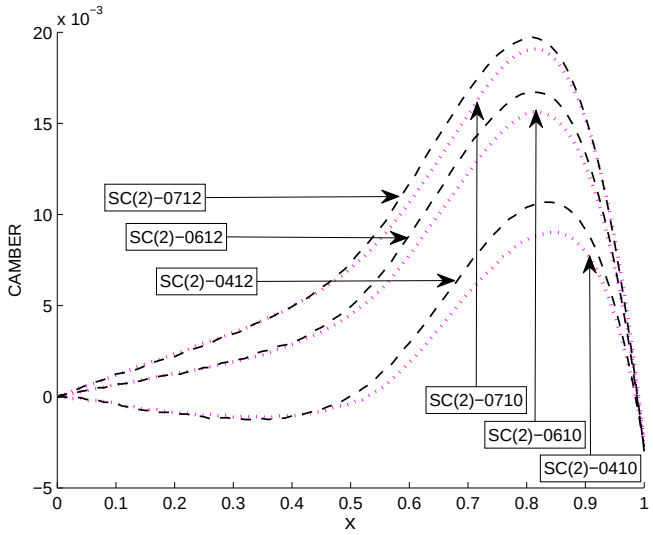

Fig. 4 The camber curves of the six SC(2) airfoils (axes to different scales).

to chord ratio and design lift coefficient – denoted as t/c and c_l respectively in what follows. The mapping we seek is therefore the first of the sequence

$$(t/c, c_l) \longmapsto \left(v_0^{\mathrm{u}}, v_1^{\mathrm{u}}, \ldots, v_{\mathrm{LE}}^{\mathrm{l}}\right) \longmapsto [z^{\mathrm{u}}(x), z^{\mathrm{l}}(x)], \tag{10}$$

where we already have the second step in the shape of equations (2) and (3).

Now, having turned our attention to separating the airfoil into camber and thickness distribution, the class-shape transformation gives us a compact way of writing these – manipulating equations (2) and (3) we get

$$\text{CAMBER}(x,\ v_0^{\text{u}},\ldots,v_{\text{TE}}^{\text{u}},\ v_0^{\text{l}},\ldots,v_{\text{TE}}^{\text{l}},) = \underbrace{\sqrt{x}(1-x)}_{\text{class function}} \underbrace{\sum_{r=0}^{n_{\text{BP}}} \frac{v_r^{\text{u}}+v_r^{\text{l}}}{2}\ C_{n_{\text{BP}}}^{\ r} x^r (1-x)^{n_{\text{BP}}-r}}_{\text{scaled Bernstein partition of unity}} +$$
$$+ \underbrace{\frac{z_{\text{TE}}^{\text{u}}+z_{\text{TE}}^{\text{l}}}{2}x}_{\text{trailing edge thickness term}} + \tag{11}$$
$$+ \underbrace{x\sqrt{1-x}\ \frac{v_{\text{TE}}^{\text{u}}+v_{\text{TE}}^{\text{l}}}{2}(1-x)^{n_{\text{BP}}}}_{\text{supplementary leading edge shaping term}},$$

and

$$\text{HT}(x,\ v_0^{\text{u}},\ldots,v^{\text{u}}u_{\text{TE}},\ v_0^{\text{l}},\ldots,v_{\text{TE}}^{\text{l}},) = \underbrace{\sqrt{x}(1-x)}_{\text{class function}} \underbrace{\sum_{r=0}^{n_{\text{BP}}} \frac{v_r^{u}-v_r^{\text{l}}}{2}\ C_{n_{\text{BP}}}^{\ r} x^r (1-x)^{n_{\text{BP}}-r}}_{\text{scaled Bernstein partition of unity}} +$$
$$+ \underbrace{\frac{z_{\text{TE}}^{\text{u}}-z_{\text{TE}}^{\text{l}}}{2}x}_{\text{trailing edge thickness term}} + \tag{12}$$
$$+ \underbrace{x\sqrt{1-x}\ \frac{v_{\text{TE}}^{\text{u}}-v_{\text{TE}}^{\text{l}}}{2}(1-x)^{n_{\text{BP}}}}_{\text{supplementary leading edge shaping term}},$$

respectively, where HT denotes half thickness (note that in order to simplify the equations we are assuming $n_{\text{BP}}^{\text{u}} = n_{\text{BP}}^{\text{l}} = n_{\text{BP}}$). This is, in fact, a variable transformation, which gives us the possibility of breaking up the required first mapping of (10) into two more easily manageable sub-problems (divide and conquer again!), the right hand one of which we have just solved:

$$(t/c, c_l) \longmapsto \left(\frac{v_0^{\text{u}}+v_0^{\text{l}}}{2}, \frac{v_0^{\text{u}}-v_0^{\text{l}}}{2}, \ldots \frac{v_{\text{LE}}^{\text{u}}-v_{\text{LE}}^{\text{l}}}{2}\right) \longmapsto \left(v_0^{\text{u}}, v_1^{\text{u}}, \ldots, v_{\text{LE}}^{\text{l}}\right) \longmapsto [z^{\text{u}}(x), z^{l}(x)], \tag{13}$$

This has not reduced the dimensionality of our design space yet, but has given us intervening variables that are more useful in terms of exploiting the separation of camber and thickness distribution and have therefore taken us closer to the ultimate goal of mapping from the $(t/c, c_l)$ space. For the final remaining step we divide the problem once more and first look at the

$$t/c \longmapsto \left(\frac{v_0^{\text{u}}-v_0^{\text{l}}}{2}, \frac{v_1^{\text{u}}-v_1^{\text{l}}}{2}, \ldots, \frac{z_{\text{TE}}^{\text{u}}-z_{\text{TE}}^{\text{l}}}{2}, \frac{v_{\text{LE}}^{\text{u}}-v_{\text{LE}}^{\text{l}}}{2}\right) \tag{14}$$

subproblem. Having already established that the thickness distribution of the six example airfoils depends only on the maximum thickness to chord ratio t/c and noting that the relationship is clearly linear, the r^{th} half thickness term in the description of the parametric airfoil will be a function of t/c as follows:

$$\left.\frac{v_r^{\text{u}}-v_r^{\text{l}}}{2}\right|_{t/c} = \frac{v_{r\sim\text{SC(2)}-0410}^{\text{u}}-v_{r\sim\text{SC(2)}-0410}^{\text{l}}}{2} +$$
$$+\left(\frac{v_{r\sim\text{SC(2)}-0412}^{\text{u}}-v_{r\sim\text{SC(2)}-0412}^{\text{l}}}{2} - \frac{v_{r\sim\text{SC(2)}-0410}^{\text{u}}-v_{r\sim\text{SC(2)}-0410}^{\text{l}}}{2}\right) \times \frac{t/c-10}{t/c-12}, \quad t/c \in [10,12]. \tag{15}$$

Note that where we used coefficients from the class-shape transformation of, say, SC(2)-0412 (for example, $v^l_{r\sim \mathrm{SC}(2)-0412}$), we could equally have used the relevant coefficients of any of the 12 % thick airfoils, as they only appear as part of the transformation coefficients of the thickness distributions, which, as we have seen, are identical for airfoils of the same maximum thickness. This, as well as the above equation, are equally applicable to the calculation of the two remaining parameters, the additional leading edge shaping term and the trailing edge thickness term.

We now need to find a way of constructing the coefficients of the camber curve transformation of the parametric airfoil, that is, to find the

$$(t/c, c_l) \longmapsto \left(\frac{v_0^{\mathrm{u}} + v_0^{\mathrm{l}}}{2}, \frac{v_1^{\mathrm{u}} + v_1^{\mathrm{l}}}{2}, \ldots, \frac{z_{\mathrm{TE}}^{\mathrm{u}} + z_{\mathrm{TE}}^{\mathrm{l}}}{2}, \frac{v_{\mathrm{LE}}^{\mathrm{u}} + v_{\mathrm{LE}}^{\mathrm{l}}}{2} \right) \tag{16}$$

part of the mapping (13). This is a slightly more complicated proposition, as the shape of the camber curve, though chiefly influenced by the design c_l, varies between airfoils of different thicknesses, as shown in Figure 4. We therefore need to construct a model of each of the camber curve parameters on the right hand side of (16) as a function of design c_l and t/c, based on the six examples provided by our chosen six SC(2) sections.

B. A Gaussian Process Model

Considering that the sets of transformation coefficients v and z we have identified earlier define *approximations* of the six 'training' airfoils (when inserted into equations (2) and (3)) and therefore the camber line coefficients are also approximations of the camber lines of the six airfoils, we shall build a *regression* model of (16) (as opposed to an interpolating one) to filter out the 'noise' in the coefficient values.

We choose to work with a Gaussian Process modeling approach – kriging – and we use the implementation described in Ref. 11. The interested reader is invited to consult this reference for the details of the formulation; here we limit ourselves to a brief summary of the problem setup.

Let us, for each camber line class-shape transformation coefficient (the right hand side of (16)), consider a 6×2 matrix $\mathbf{X}$ of the t/c ratios (column one) and design c_l values (column two) of our set of supercritical airfols and a 6×1 vector $\mathbf{y}$ of the corresponding values of the current camber transformation coefficient. We then construct a matrix $\mathbf{\Psi}$ of correlations between the 6 training points contained in $\mathbf{X}$, which is now a function of the model parameter vector θ. Additionally, to account for the inexact nature of the approximations (2) and (3) constructed with the transformation variables, we add a regression parameter λ to the leading diagonal of the correlation matrix – both θ and λ are estimated subsequently via a likelihood maximization procedure.

The kriging regression model is thus given by:

$$\hat{y}(t/c, c_l) = \hat{\mu} + \psi^{\mathrm{T}}(\mathbf{\Psi} + \lambda \mathbf{I})^{-1}(\mathbf{y} - \mathbf{1}\mu), \tag{17}$$

where

$$\hat{\mu} = \frac{\mathbf{1}^{\mathrm{T}}(\mathbf{\Psi} + \lambda \mathbf{I})^{-1}\mathbf{y}}{\mathbf{1}^{\mathrm{T}}(\mathbf{\Psi} + \lambda \mathbf{I})^{-1}\mathbf{1}}, \tag{18}$$

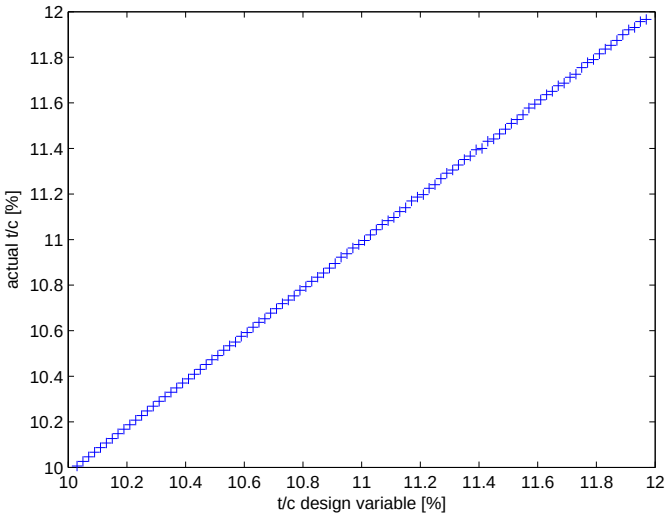

Fig. 5 Actual thickness to chord ratio versus the 't/c' design variable value across 100 airfoils spread evenly across the design space.

I is a 12×12 identity matrix and ψ is a vector containing the correlations between the training data and the $(t/c, c_l)$ pair, where we wish to predict the current class-shape transformation parameter.

The model (17) is an approximation of mapping (16) and thus completes the mapping (13). We therefore now have the complete route from $(t/c, c_l)$ to the explicit definition of the airfoil based on equations (2) and (3). This, then, is a parametric airfoil depending on two design variables, whose ranges are defined by the six airfoil training set: $t/c \in [10, 12]$, $c_l \in [0.4, 0.7]$.

C. Physical Significance

While not strictly relevant from the perspective of an automated design process, it is still natural to ask: is there a correlation between the physical properties of the new parametric airfoil we have created and the pair of design variables that control its shape?

Figures 5 and 6 depict the results of a test designed to get an insight into this question. We have generated 100 pairs of $(t/c, c_l)$ values, arranged in the $[10, 12] \times [0.4, 0.7]$ design space in a Morris-Mitchell-optimal latin hypercube sampling pattern (see Ref. 11 for details of the formulation and the algorithm used[‡]). These designs were then evaluated in terms of their maximum thickness to chord ratios (Figure 5) and their lift coefficients at M= 0.7, $\alpha = 0$ and Re= 3×10^7 (Figure 6) – the latter was computed using the ESDU VGK full potential solver.[12]

Correlation can be observed in both cases. In fact, the maximum thickness to chord ratio of the parametric airfoil can clearly be said to be equal, for most practical purposes, to the value of the 't/c' design variable. Once again, this has little significance in most automated design processes, but it can be seen as a useful feature, for example, if we want to restrict the design space to, say, wings that can

[‡]Latin hypercubes have uniform projections onto all axes and are therefore ideal for correlation studies.

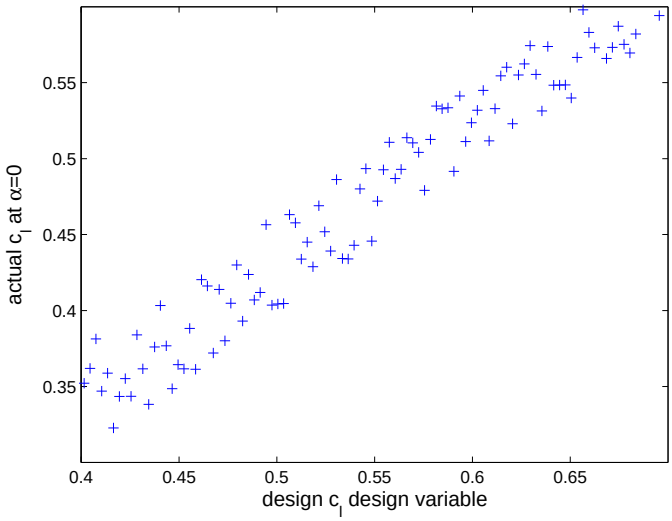

Fig. 6 Actual c_l at M0.7 and $\alpha = 0$ versus the 'c_l' design variable value across 100 airfoils spread evenly across the design space.

accommodate a certain spar depth (that is, their t/c must be greater than a certain threshold value).

Much of this study was based on the observation that we can link the design variables to easily separable elements of the airfoil shapes (crucially, we have found the thickness distributions of the six members of the family to be connected exclusively to the maximum thickness to chord value that headlines each airfoil). We look at a more general case next, where such reasoning is no longer possible.

V. A More Diverse Family

A. Patterns

Consider now a larger subset of SC(2) supercritical airfoils: SC(2)-0406, SC(2)-0606, SC(2)-0706, SC(2)-0410, SC(2)-0610, SC(2)-0710, SC(2)-0412, SC(2)-0612, SC(2)-0712, SC(2)-0414, SC(2)-0614 and SC(2)-0714. These 12 sections now encompass a broader range of design c_l values and t/c ratios then the set we analyzed earlier. The crucial difference with respect to the previous family of six is that the pattern of thickness distributions and camber curve variations within the family is considerably more complicated. We shall use this broader family to illustrate a more general form of the class-shape transformation dimensionality reduction heuristic presented earlier.

Once again we begin by approximating every member of the chosen family through its class-shape transformation. This time, we set the orders of the Bernstein polynomial terms to $n^u_{\mathrm{BP}} = 2$ and $n^l_{\mathrm{BP}} = 3$ for the upper and lower surfaces respectively. The sets of transformation coefficients of the 12 target airfoils yielded by solving equation (6) are depicted in Figure 7.

Also shown in the same figure are the 'coefficient-fingerprints' of a number of additional airfoils. It is clear that the SC(2) coefficient sets form a rather obvious 'wr'-shaped pattern, rather dissimilar to the shapes corresponding to the other airfoils (especially in the case of the 'w' corresponding to the

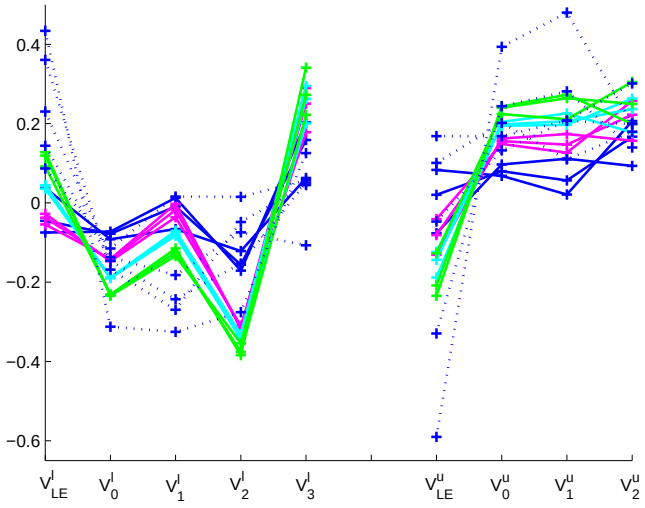

Fig. 7 Class-shape transformation coefficients of a set of well-known airfoils. The heavy, continuous lines denote the 12 SC(2) supercritical airfoils discussed here, while the dotted lines represent the approximation coefficients of NACA5410, NLR7301, RAE5215, RAE2822 and NACA24-011. Note the distinctive 'wr'-shaped pattern of the SC(2) family.

rather typical shapes of the SC(2) lower surfaces).

If we hadn't already studied a six airfoil subset of this family, the existence of this pattern would be our first indication that we are likely to need considerably fewer design variables to cover this restricted space than the 11 variables of the class-shape transformation itself (the nine shown in Figure 7, plus the two trailing edge thickness parameters). Essentially, we have to opportunity to trade flexibility for conciseness. Restricting any design searches to these 'wr'-shaped coefficient sets also has the advantage of ensuring that the design space will only contain physically 'sensible' (and 'supercritical') shapes.

As before, we shall aim to map the $t/c, c_l$ pair to the space of class-shape transformation coefficients and therefore to z^u and z^l, that is, we seek to build the first part of the mapping (10) (equations (2) and (3) form the second part).

Of course, all this reasoning on patterns is based on intuition and is the expression of certain assumptions – not least that the shapes of the SC(2) airfoils are chiefly determined by design lift coefficient and thickness and that otherwise their design generally follows the same principles across the family (this was clear in the case of our earlier, 'separable' set, but less obvious here). Additionally, we will assume separability, that is, that each class-shape transformation variable can be generated from a $(c_l, t/c)$ pair via a mapping that is independent of the other transformation variables. Intuitively, the similar shapes of the transformation variable patterns indicate that this is a reasonable assumption to make. In the case presented earlier we made, tacitly, a weaker form of this assumption: there we

could, at least, be sure of the separability of the mappings between the half-thickness coefficients and 't/c'.

The purely intuitive nature of the above, however, is of no practical significance, as long as we manage to construct a well-posed model of the mappings and the resulting reduced dimensionality airfoil is suitable for design studies. We shall return shortly to the mathematical 'checks and balances' we can use to confirm the correctness of our assumptions (at least from a practical perspective) – here we merely note that an additional bonus and further confirmation of the correctness of these assumptions would be the existence, as in the previous study, of some degree of correlation between the design variable values t/c and c_l and the maximum thickness and the lift coefficient of the resulting instantiation of our parametric airfoil.

B. Another Kriging Model

We postulated that, within the mapping (10), the individual $(t/c, c_l) \mapsto v$ mappings are considered to be separable. We can therefore attempt to build a model of each class-shape transformation coefficient v in terms of c_l and t/c, based on the 12 known pairings resulting from our approximations of the 12 SC(2) airfoils.

We no longer have any of the handholds we took advantage of in the previous case (the six airfoil family), so we have to construct 11 such models. The process employed is much the same as before – we find the model parameters by maximizing the likelihood of the data – except that on this occasion we do not build the models in terms of the intervening camber coefficient variables, but directly in terms of the variables describing the airfoil surfaces. Figure 8 is a depiction of one such model, also showing the 12 training data points, one representing each example airfoil.

If our assumption of separability was seriously wrong, this is where alarm bells would first start ringing. For instance, in the absence of a clear trend (which would imply that a third variable has a significant influence over the shapes of the airfoils) the variations within the log-likelihood landscape would be generally low and would not have clear maxima. Recall that this is a function of the the kriging model parameters (a θ per dimension and a global regression parameter λ) and the presence of significant additional factors would lead to very different combinations of these parameters being almost equally likely – clearly a sign that there are no trends in the data. Should the reader opt for other methods of determining the the θ's and λ, these are usually also equipped with warning devices that will indicate if the initial assumptions are wrong. For example, leave-k-out cross-validation[11] would yield cross-validation errors per data point comparable to the range of the responses – again, a sign that other factors have a significant impact on the data[§].

C. Physical Relevance

As before, a space-filling set of designs was generated and tested from the point of view of the accuracy of our approximation of mapping (10). Figure 9 shows that, as before, the t/c design variable

[§]We stress the word 'significant' here for a good reason – in the process of tailoring the SC(2) airfoils small shape alterations *were* necessary in some cases to obtain the desired pressure profiles (in particular shock locations) and drag rise Mach numbers, but, for practical purposes, we can assume that the two major factors with consistently significant impact were t/c and the desired c_l.

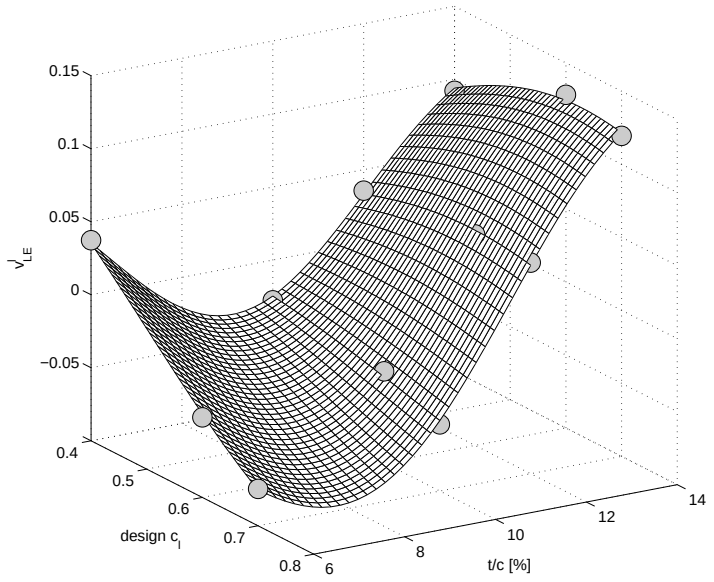

Fig. 8 Gaussian Process regression model of the value of one of the class-shape transformation parameters (v^l_{LE}), trained on the 12 values found as optimal for the set of SC(2) airfoils.

is virtually equal to the maximum thickness to chord ratio of the airfoil the mapping will generate. A weaker correlation can be observed in terms of the c_l variable (Figure 9)– here we can also see a loss of approximation accuracy compared to the first case.

Figure 11 is a further illustration of the physical significance of the design variables: different values of the c_l variable produce airfoils with variable camber (left), while the camber is maintained and the thickness changes as t/c varies (right).

VI. Reflections on the Design Process

So what does all this mean from the perspective of the preliminary design process[¶]? In the above we have described the construction of a parametric airfoil defined by two design variables. The process illustrated above for the family of SC(2) supercritical airfoils can be employed to exploit patterns in the class-shape transformation coefficients of other families of similar airfoils. This reduced dimensionality model can then be used for global design searches, safe in the knowledge that we have minimized the contribution of the airfoil to the overall dimensionality of the airframe geometry.

Once this first step of the optimization process is complete, we are left with an airfoil expressed in the form of equations (2) and (3), i.e., as a Kulfan transformation, which can form the starting point of a subsequent local search. This second optimization procedure can then exploit the aerodynamic

[¶]We choose to define as 'preliminary' the phase of the first step of the design process that is centered around a geometry.

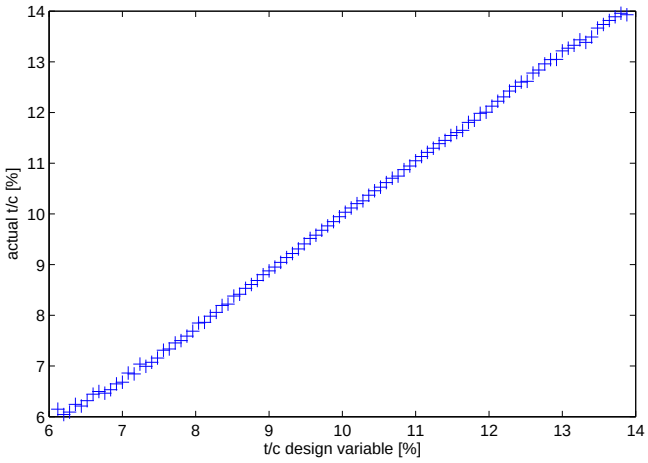

Fig. 9 Actual thickness to chord ratio versus the 't/c' design variable value across 100 airfoils spread evenly across the design space.

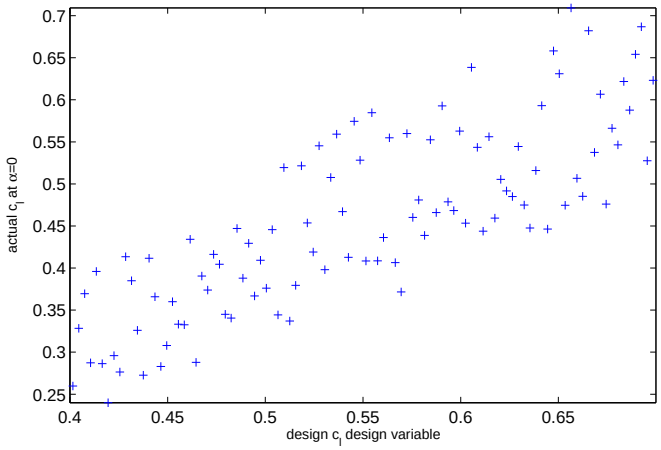

Fig. 10 Actual c_l at M0.7 and $\alpha = 0$ versus the 'c_l' design variable value across 100 airfoils spread evenly across the design space.

significance of some of the class-shape transformation variables (e.g., the first term is related to leading edge radius, the r^{th} controls the boattail angle), or can simply allow an automated optimizer to exploit the current basin of attraction in terms of some design goal.

VII. Conclusions and Future Work

The process described here is intended to be a possible template for the solution of a more general question, that could be phrased as follows. Let us consider a set of curves (or surfaces), which represent a diverse range of feasible (though not necessarily optimal) solutions to a design problem. What is

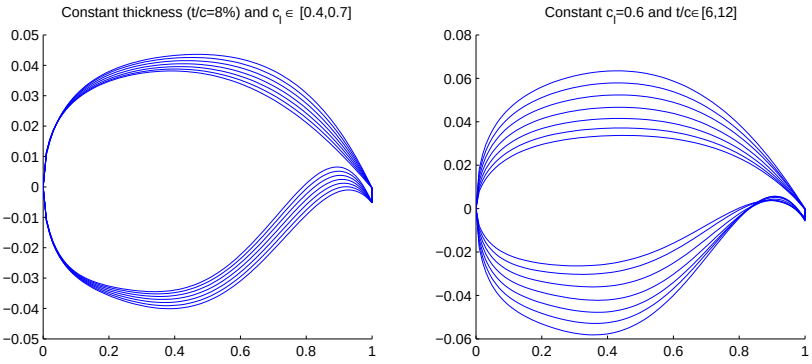

Fig. 11 Examples of instances of our two variable parametric airfoil.

the minimum dimensionality of a parametric curve (or surface) that can reproduce all of the sample curves (or surfaces) to within a specified level of accuracy, while also creating a smooth subspace of designs defined in terms of these 'training' examples?

In a previous paper[13] we have approached the problem using a NURBS description. Here we have shown the Kulfan transformation to be another feasible way of capturing the training cases and building the parametric geometry model – at least for the specific case of supercritical airfoils. We have constructed two parametric airfoils that distil the aerodynamic reasoning behind the designs of their respective subsets of training airfoils down to two design variables. Moreover, in both cases the two design variables show strong correlations with physical parameters (geometrical and aerodynamic) of the parametric airfoil, whose shape they determine, a feature that can be useful in the context of human interventions in the design process (as opposed to a purely automated search for a shape that optimizes some goal function).

Future work therefore should consider applying either strategy to broader (or different) classes of shapes. As this study indicates, the method has the potential to parameterize very complex shapes very concisely. Clearly, the design spaces generated in this way will generally be narrower (which may actually be beneficial in terms of excluding unrealistic shapes) – this potential reduction in flexibility will always have to be balanced against the 'curse of dimensionality' often brought on by the large number of design variables associated with more conventional, more flexible schemes.

Acknowledgements

The author would like to thank the Royal Academy of Engineering and the Engineering and Physical Sciences Research Council (EPSRC) for the financial support of this work.

References

[1]Sóbester, A., "Concise Airfoil Representation via Case-Based Knowledge Capture," *AIAA Journal*, Vol. 47, No. 5, 2009, pp. 1209–1218.

[2]Jameson, A., "Aerodynamic Design via Control Theory," *Journal of Scientific Computing*, Vol. 3, No. 3, 1988, pp. 233–260.

[3]Robinson, G. M. and Keane, A. J., "Concise Orthogonal Representation of Supercritical Airfoils," *Journal of Aircraft*, Vol. 38, 2001, pp. 580–583.

[4]Vanderplaats, G. N., *Numerical optimization techniques for engineering design : with applications*, McGraw-Hill, New York, 1984.

[5]Collins, L. and Saunders, D., "PROFILE: Airfoil Geometry Manipulation and Display," Contractor Report 177332, NASA, 1997.

[6]Kulfan, B. M., "Universal Parametric Geometry Representation Method," *Journal of Aircraft*, Vol. 45, No. 1, 2008, pp. 142–158, DOI: 10.2514/1.29958.

[7]Kulfan, B. M., ""Fundamental" Parametric Geometry Representations for Aircraft Component Shapes," *AIAA 2006-6948*, 2006, pp. 1–45.

[8]Harris, C. D., "NASA Supercritical Airfoils – A Matrix of Family-Related Airfoils," Technical Paper 2969, NASA, 1990.

[9]Whitcomb, R. T. and Clark, L. R., "An Airfoil Shape for Efficient Flight at Supercritical Mach Numbers," Technical Report TM X-1109, NASA, 1965.

[10]Whitcomb, R. T., "Review of NASA Supercritical Airfoils," *The Ninth Congress of the International Council of the Aeronautical Sciences*, Vol. ICAS 74-10, 1974.

[11]Forrester, A. I. J., Sóbester, A., and Keane, A. J., *Engineering Design via Surrogate Modelling*, John Wiley and Sons, 2008.

[12]Freestone, M. M., "VGK Method for Two-Dimensional Airfoil Sections," Technical report, Engineering Sciences Data Unit, 1996.

[13]Sóbester, A., "Concise Airfoil Representation via Case-Based Knowledge Capture," *AIAA Journal*, Vol. 47, No. 5, 2009, pp. 1209–1218.